

Entanglement percolation in random quantum networks

Alessandro Romancino¹ , Jordi Romero-Pallejà² , G. Massimo Palma¹  and Anna Sanpera^{2,3} 

¹ Dipartimento di Fisica e Chimica “E. Segrè”, Università degli Studi di Palermo, Via Archirafi 36, 90123 Palermo, Italy

² Grup d’Informació Quàntica, Departament de Física, Universitat Autònoma de Barcelona, 08193 Bellaterra, Spain

³ ICREA, Pg. Lluís Companys 23, 08010 Barcelona, Spain

E-mail: alessandro.romancino@unipa.it

Abstract. Entanglement percolation aims at generating maximal entanglement between any two nodes of a quantum network by utilizing strategies based solely on local operations and classical communication between the nodes. As it happens in classical percolation theory, the topology of the network is crucial, but also the entanglement shared between the nodes of the network. In a network of identically partially entangled states, the network topology determines the minimum entanglement needed for percolation. In this work, we generalize the protocol to scenarios where the initial entanglement shared between each two nodes of the network is not the same but has some randomness. In such cases, we find that for classical entanglement percolation, only the average initial entanglement is relevant. In contrast, the quantum entanglement percolation protocol generally performs worse under these more realistic conditions.

Keywords: quantum networks, entanglement, quantum information, quantum internet, percolation, stochastic locc, random states, entanglement distribution

1. Introduction

Despite major advances in quantum technologies, achieving reliable and efficient entanglement distribution across distant nodes of a quantum network (QN) remains one of the most challenging tasks today. Nevertheless, several real-world implementations of quantum networks have recently been demonstrated on various scales [1–5].

Establishing distributed entanglement is a crucial ingredient for the future Quantum Internet [6, 7], as well as for protocols involving conference key agreement (CKA) [8], quantum federated learning [9], quantum cryptography [10, 11], superdense coding [12], secure quantum key distribution [13] and quantum teleportation [14]. However, due to unavoidable environmental decoherence, the creation of reliable pairwise entanglement at large distances remains a difficult experimental endeavor [15, 16].

To overcome these limitations, inherent to quantum channels, quantum repeaters have been proposed as a way to achieve perfect pairwise entanglement distribution in one dimensional topologies [17–19]. In quantum repeaters, a chain of intermediate nodes act as repeaters of maximally entangled states by applying entanglement swapping [20,21]. Another protocol to achieve maximal entanglement is the so-called entanglement distillation [22–25], where multiple copies of a partially entangled state are distilled into a smaller number of maximally entangled states. Both methods, however, show fundamental limitations [26, 27], regarding the action of noise or fidelity. Recently, multiplexing entanglement sharing has also been developed as a way to distribute entanglement [28].

Here, we will focus on an alternative approach based on percolation on quantum networks called entanglement percolation [29–36]. A quantum network consist on a set of nodes (users) capable of performing local operations, and the edges (or links) corresponds to partially entangled pairs shared between the nodes [37]. The goal of entanglement percolation is to establish a maximally entangled state between two arbitrary nodes of a network, when the nodes are connected with partially entangled states. The entanglement transport (percolation) on the network depends non-trivially on the network topology (degree of connectivity fo the nodes) and on the amount on initial entanglement, typically assumed to be homogeneous across all links.

We briefly review what are the classical and quantum entanglement percolation protocols, which are the crucial concepts regarding percolation in quantum networks. The classical entanglement percolation (CEP) protocol starts from a quantum network whose edges consist of identical partially entangled bipartite states.[‡] The strategy is then to “gamble with entanglement” by applying stochastic local operations and classical communication (SLOCC). The effect of SLOCC is that each edge connecting a pair of nodes is converted into a maximally entangled pair with probability p ; otherwise, the edge is removed from the network with probability $1 - p$. This procedure maps the problem onto the classical percolation model familiar from statistical physics [38]. Every lattice then exhibits a corresponding percolation threshold.

A more efficient protocol is the so-called quantum entanglement percolation (QEP) one. In this case, each node of the network is preprocessed using some quantum operations, for instance performing entanglement swapping via “ q -swaps” operations [30]. In doing so, the original lattice structure is transformed into some other lattice for which the percolation threshold is lower [29]. The change in network topology results into an efficiency bound that can be much better than the original CEP. However, the optimal protocol for quantum entanglement percolation on a given network remains still an open question [33], and heuristics can be used to optimize it in some capacity [39].

To the best of our knowledge, entanglement percolation has been explored using pure bipartite qubits [29], mixed states [40, 41], multipartite entangled states [42, 43], noisy channels [44]. However, in all the the above cases, the edges of the quantum

[‡] In the original paper [29], the term “classical” is used purely as an analogy with classical percolation theory; the protocol itself is not classical.

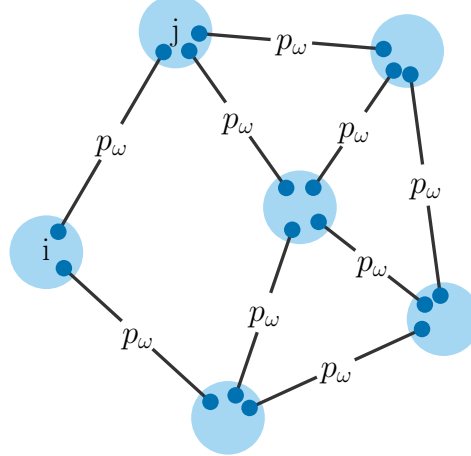


Figure 1: Example of a quantum network consisting of identical copies of state $|\omega\rangle$ with Singlet Conversion Probability (SCP) $p_\omega = 2\lambda_2^\omega$. Nodes i and j are highlighted.

network are assumed to be identical. Here, we focus on the efficiency of entanglement percolation for the more realistic scenario in which the degree of entanglement corresponding to the edges is randomly distributed.

The structure of the article is as follows: in Section 2, we introduce the main concepts underlying the entanglement percolation protocol as originally proposed in Acín *et al.* [29]. We then review the basis of the CEP protocol and the QEP protocol. In Section 3, we extend the previous analysis to networks with nonidentical shared initial states. We present our results CEP in Section 3.1 and for QEP in Section 3.2. In Section 4, we summarize our findings and open questions. For completeness, a brief overview on classical percolation theory is present in Appendix A while some formulas and results from LOCC theory are outlined in Appendix B.

2. Entanglement percolation in quantum networks

A quantum network can be modeled as a graph $G = (V, E)$, where the vertices V represent nodes (users) capable of local quantum operations, and the edges E represent bipartite quantum states shared between pairs of nodes. Each edge is associated with a partially entangled two-qubit state. In Fig. 1, a network whose edges consist on partially entangled two-qubit states, $|\omega\rangle$, is shown. Users are allowed to use local operations and classical communication (LOCC) to achieve singlets $|\Psi^-\rangle$, between two arbitrary nodes of the quantum network. Using the Schmidt decomposition of a shared bipartite pure state $|\omega\rangle = \lambda_1^\omega |00\rangle + \lambda_2^\omega |11\rangle$ (with $\lambda_2^\omega \leq \lambda_1^\omega$), together with stochastic majorization [45], it can be shown that any such state can be transformed into a singlet (or equivalently into any maximally entangled Bell state) by means of LOCC with the singlet conversion probability (SCP) $p_\omega = \min\{1, 2\lambda_2^\omega\}$. See Appendix B for the derivation details.

To achieve entanglement distribution one make use of only of two types of local operations and classical communication protocols, namely SLOCC purification and

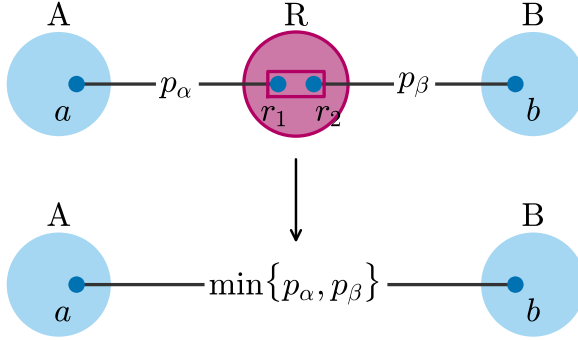


Figure 2: Representation of an entanglement swapping procedure, where a joined bell measurement is performed on systems R_1 and R_2 .

entanglement swapping.

- **SLOCC purification:** nodes i and j are connected by a partially entangled state $|\omega\rangle_{ij}$ (like in Figure 1). The optimal SLOCC purification protocol is applied on the qubits of nodes i and j . This operation, as explained in Appendix B, converts the state $|\omega\rangle_{ij}$ into the singlet $|\psi^-\rangle_{ij}$ with finite probability p_ω or, if unsuccessful, into a product state with probability $1 - p_\omega$.
- **Entanglement swapping:** as shown in Fig 2, two nodes A and B are connected with an intermediate node R , sharing states $|\alpha\rangle_{ar_1}$ and $|\beta\rangle_{br_2}$. Then, a joined Bell measurement is performed on node R by measuring systems r_1 and r_2 . This creates a new entangled state between A and B , while the node R is removed. Considering that the singlet conversion probability SCP are p_α and p_β respectively, one end up with a state with an SCP of $p_{\text{swap}} = \min\{p_\alpha, p_\beta\}$, also called “entanglement of single pair purification” [21, 46]. In this section we consider just the case where $p_\alpha = p_\beta = p$ for all the links. However, as we will see, the role of different p_i will, instead, be crucial in Section 3.2.

2.1. Classical Entanglement Percolation

The Classical Entanglement Percolation (CEP) protocol [29] consists on the following procedure:

- (i) The optimal SLOCC purification operation is applied to each link in the network. The links are either successfully converted into a singlet with probability p_ω or removed from the network (Fig. 3a).
- (ii) If the initial SCP is high enough, a chain of singlets connecting the desired nodes is created. In this case, entanglement swapping is applied in the intermediate nodes, generating the final desired singlet, as shown in Fig. 3b.

The classical theory of percolation states that if the initial p_ω is high enough there will always exist (for a large enough network) a path connecting any two pair of nodes.

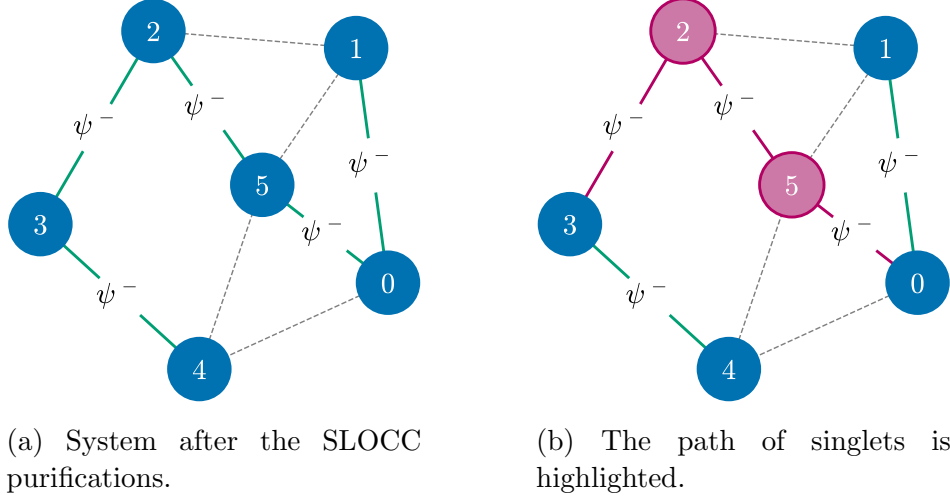


Figure 3: A single (successful) run of a classical entanglement percolation protocol. The final singlet is created between node 0 and node 3 after applying entanglement swapping on nodes 2 and 5.

This means that for entanglement percolation to be successful, it is required for the initial states to have an initial SCP $p_\omega > p_c$, where p_c is the percolation threshold of the original network [29, 30].

This threshold is called Classical Entanglement Percolation (CEP), in analogy with the classical theory of percolation [31–34]. For example, a square lattice quantum network will require states with $p_\omega > p_c^{\text{square}} = 1/2$ [47], that is, $p_{\text{square}}^{\text{CEP}} = 1/2$. The percolation threshold depends only on the network topology, and different types of complex networks can show very significant differences in the percolation threshold as shown in [30, 38, 48].

2.2. Quantum Entanglement Percolation

It has been shown that the CEP protocol is not optimal for many Quantum Networks [29, 30]. In those cases, a better performance can be achieved with the Quantum Entanglement Percolation (QEP) protocol. The starting setup for this protocol consists in a “multigraph quantum network”, that is, a quantum network where each pair of nodes can share multiple bipartite states (see Appendix C for a detailed explanation) and implement a procedure called “ q -swap”. It consists of applying entanglement swapping operations in nodes at the center of a star subgraph S_q transforming it into a C_q cycle, as can be seen in Fig. 4. These operations change the topology of the network, modifying the percolation threshold drastically [30, 49].

Therefore, in the QEP protocol, first the network is preprocessed applying appropriate q -swaps, and then the CEP protocol is applied on the new network.

As a paradigmatic example [29], starting with a double-bond honeycomb lattice, as shown in Fig. 5, by applying the CEP protocol, knowing that $p_c^{\text{hexagon}} = 1 - 2 \sin(\pi/18)$

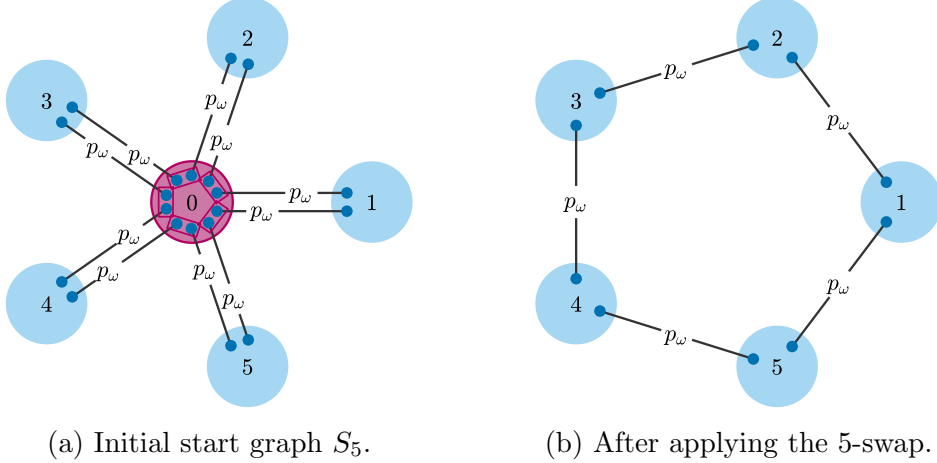


Figure 4: An example of a 5-swap operation. (a) Initial star graph S_5 with a central node 0 connected with two identical states $|\omega\rangle$ with each of the other nodes. (b) End result after performing the 5-swap between the 0 node and all other nodes. This creates new entangled states between the external nodes and erases node 0 from the network.

[50], one obtains:

$$p^{\text{CEP}} = 2 \left[1 - \sqrt{\frac{1}{2} + \sin\left(\frac{\pi}{18}\right)} \right] \approx 0.358 \quad (1)$$

If, instead we apply the QEP protocol, one initially performs 3-swaps and ends up with the triangular lattice, as shown in Fig. 5, which has $p_c^{\text{triangle}} = 2 \sin(\pi/18)$ [50]. This means that:

$$p^{\text{QEP}} = p_c^{\text{triangle}} = 2 \sin(\pi/18) \approx 0.347 \quad (2)$$

In the case here illustrated, the difference the CEP and QEP is small, but the QEP protocol can yield much better improvements in complex quantum networks [30, 49].

It is also known that QEP is not optimal. Given an arbitrary network, the order of the entanglement swapping and stochastic purification process can be tailored to the specific network, going beyond the QEP performance. It is still unknown if, given any quantum network, there exists a lower bound for initial entanglement below which it is impossible to entangle two distant qubits using only LOCC [33].

3. Entanglement percolation in random quantum networks

Entanglement percolation protocols have been extended to networks of multipartite states [42] and to networks of mixed states [40]. Here, we analyze a still unexplored but highly relevant and realistic scenario: a random quantum network (RQN). In this setting, we relax the usual assumption that all initially shared quantum states are identical and instead assume a statistical distribution of the initial SCPs

Let the k -th edge state be $|\psi_k\rangle$, the SCP of the k -th edge will be $p_k = 2\lambda_2^{\psi_k}$ where $\lambda_2^{\psi_k}$ is the smallest Schmidt coefficient of the state $|\psi_k\rangle$. In the following, we assume

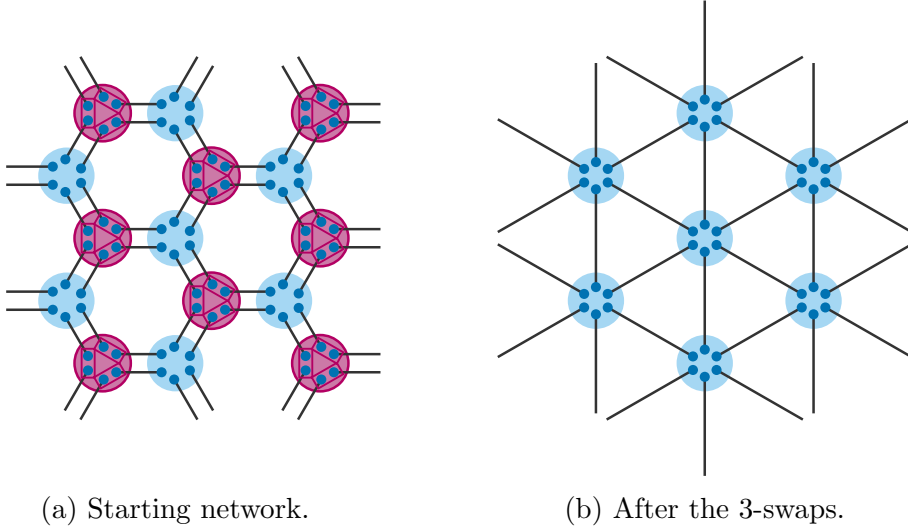


Figure 5: Representation of the initial and final networks after applying the QEP protocol to a double-bond honeycomb lattice.

that p_k are randomly distributed, as illustrated in Fig. 6a. We stress here that such situation represents a more generic case than just having random Haar distributed states of bipartite qubit pairs [51, 52]. Notice that Haar states are associated with a unique distribution of Schmidt coefficients [53, 54], meaning that Haar distributed states are just one particular example of all possible distributions of Schmidt coefficients.

In particular, the distribution shown in Fig. 6b of the smallest Schmidt coefficients, λ_2 , of a Haar random state of a pair of qubits, is:

$$p(\lambda_2) = 6(1 - 2\lambda_2)^2 \quad (3)$$

which leads to $\langle \lambda_2 \rangle = \frac{1}{8}$. This means that the average SCP of a random Haar state is $\langle p_{\text{Haar}} \rangle = \frac{1}{4}$.

3.1. CEP in RQN

The implementation of the CEP protocol to this new random quantum networks is straightforward: the optimal SLOCC is applied to each edge (each of which will now have a different probability of success) and then, if the initial amount of entanglement is high enough, there will always exist a path of singlets between two given nodes.

As an example, a uniform distribution for the SCPs has been assumed::

$$\chi(p) = \begin{cases} \frac{1}{b-a} & \text{for } a \leq p \leq b \\ 0 & \text{elsewhere} \end{cases} \quad (4)$$

with average value of $\langle p \rangle = \frac{a+b}{2}$ and width $w = b-a$ with $0 \leq a < b \leq 1$. Several random quantum network CEPs have been simulated, with the width w and the average value $\langle p \rangle$ serving as control parameters. For each parameter set, multiple realizations of the

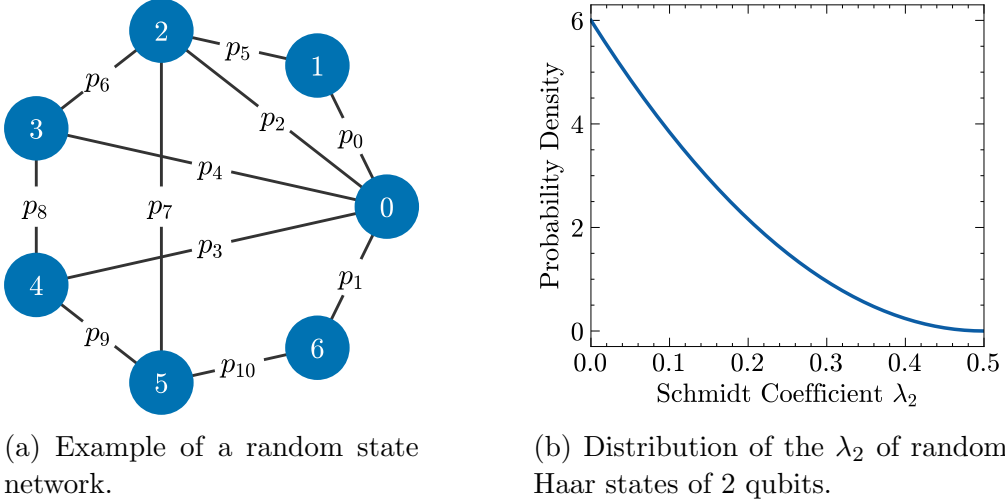


Figure 6: Examples for a random state network. The Haar random states make up a particular distribution from all the possible ones.

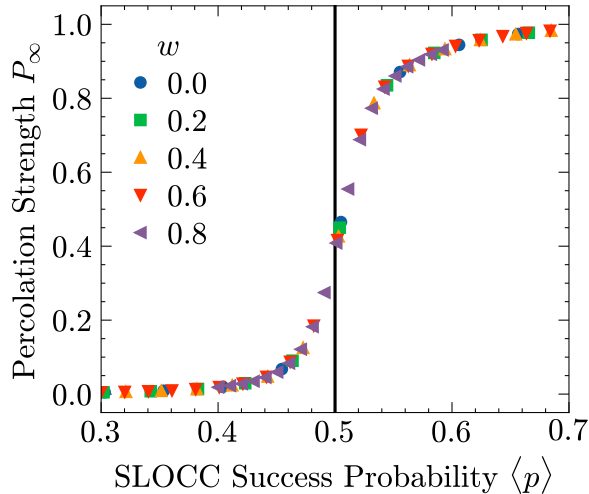


Figure 7: Simulation for the entanglement percolation in a random quantum network. The percolation strength is shown as the order parameter for the transition by changing the SLOCC success probability $\langle p \rangle = \frac{a+b}{2}$. The simulation was done in a 100×100 square lattice, the percolation threshold $p_c^{\text{square}} = 0.5$ is shown as a black vertical line. The simulation was done for $w = 0, 0.2, 0.4, 0.6, 0.8$.

same network – specifically, a 100×100 square lattice – were generated and simulated. From these simulations, the Percolation strength P_∞ ; i.e., which is the probability of a random node belonging to the biggest cluster of connected nodes, was computed (see Appendix A for details) [55].

As shown in Fig. 7, the results obtained for the different simulations are identical width-wise. This implies that only the average value of the distribution is relevant for CEP, or, in other words, that only the average initial entanglement is important, as

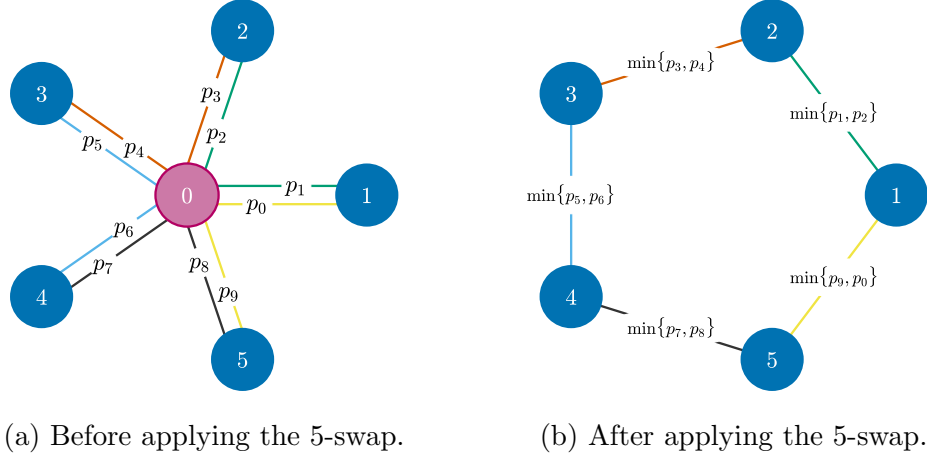


Figure 8: A 5-swap applied to a random state network with random multiedges.

happens when all the edges of the network have the same SCP. Therefore, if the average initial SCP is above the classical percolation threshold p_c then the system percolates, otherwise it does not:

$$p_{\text{rand}}^{\text{CEP}} = p_c \quad (5)$$

We obtained the same results for different initial network topologies (Erdős–Rényi and Watts–Strogatz networks) and for different distributions of the SCPs (truncated gaussian and bimodal distribution, both symmetric and asymmetric).

3.2. QEP in RQN

In this section we will proceed to compare the efficiency of the QEP protocol and the CEP protocol with random quantum networks. Nevertheless, the q -swap defined in Section 2.2 has to be generalized before proceeding with the protocols comparison. A known result is that entanglement swapping between two states with SCPs p_{k_1} and p_{k_2} yields a new state with an SCP equal to $\min\{p_{k_1}, p_{k_2}\}$ [21]. This means that the q -swaps now not only modify the topology of the network, but now also the distribution of the SCPs, as shown in Fig. 8.

In the new random quantum network after the q -swaps operations the distribution of the SCPs corresponds to the distribution of the minimum of two independent and identically distributed variables (IID).

This concept of the “distribution of the minimum” is common in the field of extreme value theory [56]. In particular, given $Y = \min\{X_1, X_2\}$ and using the cumulative distribution function F_{\min} :

$$F_{\min}(x) = P(Y \leq x) = P(\min\{X_1, X_2\} \leq x) = 1 - P(X_1 > x, X_2 > x) \quad (6)$$

due to the fact that only one $X_i \leq x$ is required. However, the X_i are IIDs and, therefore, $P(X_1 > x, X_2 > x) = [1 - F(x)]^2$ where $F(x) = P(X_i \leq x)$. This leads to a formula for

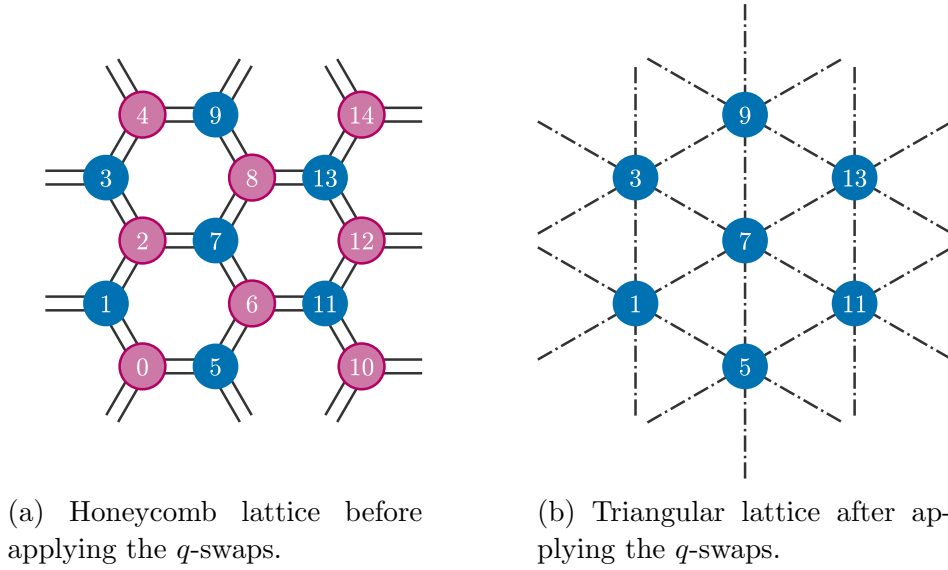


Figure 9: Honeycomb to triangular lattice transformation obtained after applying the q -swaps in the nodes highlighted in red. The edges in the newly formed triangular lattice have the SCP following the distribution of the minimum (shown as dotted line in the figure).

the probability density function:

$$f_{\min}(x) = 2f(x)[1 - F(x)] \quad (7)$$

For example, calculating the distribution of the minimum of two IID from the uniform distribution in Equation (4). By using Equation (7), we get the following distribution

$$\chi_{\min}(p) = \begin{cases} \frac{2}{b-a} \left(1 - \frac{p-a}{b-a}\right) & \text{for } a \leq p \leq b \\ 0 & \text{elsewhere} \end{cases} \quad (8)$$

with average value:

$$\langle p_{\min} \rangle = \langle p \rangle - w/6 \quad (9)$$

This is a reasonable result, the wider the uniform distribution is, the more skewed to the left the distribution of the minimum will be, yielding a lower average.

We now analyze the example of a double-bond honeycomb network (like the one in Section 2.2) with uniformly distributed SCPs. Combining Equation (5) and $\langle p_{k_1 \otimes k_2} \rangle = p_c^{\text{hexagon}}$ (see Appendix D for more details), the CEP for this network becomes

$$p_{\text{rand}}^{\text{CEP}} = 2 \left[1 - \sqrt{\frac{1}{2} + \sin\left(\frac{\pi}{18}\right)} \right] \approx 0.358 \quad (10)$$

Applying instead the QEP protocol; i.e., transforming the double-bond honeycomb lattice into a triangular lattice with the distribution of the minimum, we obtain that

$\langle p_{\min} \rangle = p_c^{\text{triangle}}$. Using Equation (9), it can be seen that:

$$p_{\text{rand}}^{\text{QEP}} = 2 \sin\left(\frac{\pi}{18}\right) + \frac{w}{6} \approx 0.347 + \frac{w}{6} \quad (11)$$

which now depends on the width of the distribution.

Equation (11) shows that the wider the distribution, the worse the performance of the QEP protocol is, at variance with the CEP protocol which instead does not depend on the width of the distribution. This means that there exists a threshold w^* after which $p_{\text{rand}}^{\text{CEP}} < p_{\text{rand}}^{\text{QEP}}$. For instance, for $w < w^* \approx 0.067$ the QEP protocol is more optimal than CEP for the studied lattice while for $w > w^*$ the protocol is instead disadvantageous.

In general, for the networks studied in this work, the CEP protocol performs better when the underlying distribution is wide. Moreover, we conjecture that this behavior is generic for random quantum networks and that, consequently, there exists a width threshold, w^* , which may be interpreted as a distribution with sufficient noise, above which the CEP protocol becomes more optimal than QEP.

4. Conclusions

We have generalized the entanglement percolation protocol in quantum networks to the more realistic scenario in which the degree of entanglement between nodes is randomly distributed. Assuming a distribution of states with random Schmidt coefficients we have found that only the average value of the initial entanglement is important for classical entanglement percolation, mapping again the problem to the classical percolation transition. By applying, instead, the quantum entanglement percolation protocol we found that random quantum networks yield different results than before. Surprisingly, we have shown that with these realistic scenario, quantum local operations are disadvantageous for entanglement distribution. This means that, with random state quantum networks the classical entanglement percolation (CEP) protocol performs better than the quantum one (QEP). We conjecture that for “noisy” networks the CEP protocol is the best possible protocol for entanglement distribution using LOCC.

Applying this framework to the multipartite case might be promising, as the non-random model shows a big improvement over the bipartite case. This is done by mapping the hypergraph representation into a bipartite graph and then analyzing node percolation of the said graph [42]. A true full hypergraph percolation theory is still being investigated [57]. Another approach, called concurrence percolation [58–61] has also been showing promising results and this generalization can be applied to that framework as well. Still, whether it exist a minimum amount of initial entanglement needed in order to achieve a perfect long distance entanglement is still unknown.

Acknowledgments

GMP acknowledges support by MUR under PRIN Project No. 2022FEXLYB, Quantum Reservoir Computing (QuReCo). AR acknowledges the grant “Bando Viaggi e Soggiorni

di Studio degli Studenti - Anno 2022" from Università degli Studi di Palermo. JRP acknowledges financial support from the Spanish MICIN FPU22/01511. AS and JRP acknowledges financial support from Ministerio de Ciencia e Innovación of the Spanish Government with funding from European Union NextGenerationEU (PRTR-C17.I1) and by Generalitat de Catalunya and from the Spanish MICIN (project PID2022-141283NB-I00) with the support of FEDER funds, and by the Ministry for Digital Transformation and of Civil Service of the Spanish Government through the QUANTUM ENIA project call - Quantum Spain project, and by the European Union through the Recovery, Transformation and Resilience Plan - NextGeneration EU within the framework of the Digital Spain 2026 Agenda.

References

- [1] Ramakrishnan R K *et al.* 2023 *Journal of the Indian Institute of Science* **103** 547–467
- [2] Wei S H *et al.* 2022 *Laser & Photonics Reviews* **16** 2100219
- [3] Joshi S K *et al.* 2020 *Science Advances* **6** eaba0959
- [4] Brekenfeld M, Niemietz D, Christesen J D and Rempe G 2020 *Nature Physics* **16** 647–651
- [5] Thomas S E, Wagner L, Joos R, Sittig R, Nawrath C, Burdekin P, de Buy Wenniger I M, Rasiah M J, Huber-Loyola T, Sagona-Stophei S *et al.* 2024 *Science Advances* **10** eadi7346
- [6] Kimble H J 2008 *Nature* **453** 1023–1030
- [7] Wehner S, Elkouss D and Hanson R 2018 *Science* **362** eaam9288
- [8] Murta G, Grasselli F, Kampermann H and Bruß D 2020 *Advanced Quantum Technologies* **3** 2000025 (arXiv:<https://advanced.onlinelibrary.wiley.com/doi/pdf/10.1002/quate.202000025>) URL <https://advanced.onlinelibrary.wiley.com/doi/abs/10.1002/quate.202000025>
- [9] Nguyen D C, Uddin M R, Shaon S, Rahman R, Dobre O and Niyato D 2025 Quantum federated learning: A comprehensive survey (arXiv:2508.15998) URL <https://arxiv.org/abs/2508.15998>
- [10] Ekert A K 1991 *Physical Review Letters* **67** 661–663
- [11] Bennett C H and Brassard G 1991 *Theoretical Computer Science* **560** 7–11
- [12] Bennett C H and Wiesner S J 1992 *Physical Review Letters* **69** 2881–2884
- [13] Lo H, Curty M and Tamaki K 2014 *Nature Photonics* **8** 595–604 ISSN 1749-4885, 1749-4893 URL <https://www.nature.com/articles/nphoton.2014.149>
- [14] Bennett C H, Brassard G, Crépeau C, Jozsa R, Peres A and Wootters W K 1993 *Physical Review Letters* **70** 1895–1899
- [15] Yin J *et al.* 2017 *Science* **356** 1140–1144
- [16] Neumann S P, Buchner A, Bulla L, Bohmann M and Ursin R 2022 *Nature Communications* **13** 6134
- [17] Briegel H J, Dür W, Cirac J I and Zoller P 1998 *Physical Review Letters* **81** 5932–5935
- [18] Cirac J I, Zoller P, Kimble H J and Mabuchi H 1997 *Physical Review Letters* **78** 3221
- [19] Dür W, Briegel H J, Cirac J and Zoller P 1999 *Physical Review A* **59** 169–181
- [20] Żukowski M, Zeilinger A, Horne M A and Ekert A K 1993 *Physical Review Letters* **71** 4287–4290
- [21] Bose S, Vedral V and Knight P L 1999 *Physical Review A* **60** 194–197
- [22] Bennett C H, Brassard G, Popescu S, Schumacher B, Smolin J A and Wootters W K 1996 *Physical Review Letters* **76** 722–725
- [23] Bennett C H, Bernstein H J, Popescu S and Schumacher B 1996 *Physical Review A* **53** 2046–2052
- [24] Bennett C H, DiVincenzo D P, Smolin J A and Wootters W K 1996 *Physical Review A* **54** 3824–3851

- [25] Deutsch D, Ekert A, Jozsa R, Macchiavello C, Popescu S and Sanpera A 1996 *Physical Review Letters* **77** 2818–2821
- [26] Pirandola S, Laurenza R, Ottaviani C and Banchi L 2017 *Nature communications* **8** 1–15
- [27] Winnel M S, Guanzon J J, Hosseinidehaj N and Ralph T C 2022 *npj Quantum Information* **8** 129
- [28] Ruskuc A, Wu C J, Green E, Hermans S L N, Pajak W, Choi J and Faraon A 2025 *Nature* **639** 54–59 ISSN 1476-4687
- [29] Acín A, Cirac J I and Lewenstein M 2007 *Nature Physics* **3** 256–259
- [30] Cuquet M and Calsamiglia J 2009 *Physical Review Letters* **103** 240503
- [31] Perseguers S, Cirac J I, Acín A, Lewenstein M and Wehr J 2008 *Physical Review A* **77** 022308
- [32] Lapeyre G J, Wehr J and Lewenstein M 2009 *Physical Review A* **79** 042324
- [33] Perseguers S, Lapeyre G J, Cavalcanti D, Lewenstein M and Acín A 2013 *Reports on Progress in Physics* **76** 096001
- [34] Siomau M 2016 *Journal of Physics B: Atomic, Molecular and Optical Physics* **49** 175506
- [35] Meng X, Hu X, Tian Y, Dong G, Lambiotte R, Gao J and Havlin S 2023 *Entropy* **25** 1564
- [36] Wang C, Hu X and Dong G 2024 *Mathematics* **12** 3568 ISSN 2227-7390
- [37] Biamonte J, Faccin M and De Domenico M 2019 *Communications Physics* **2** 53
- [38] Newman M 2018 *Networks (2nd Edition)* (Oxford University Press)
- [39] De Girolamo A, Magnifico G and Lupo C 2025 *Quantum Science and Technology* **10** 035047 ISSN 2058-9565
- [40] Broadfoot S, Dorner U and Jaksch D 2009 *Europhysics Letters* **88** 50002
- [41] Wang H, Malik O, Hou J, Zhang Y, He K and Meng X 2026 *Communications Physics* **9** 28 ISSN 2399-3650
- [42] Perseguers S, Cavalcanti D, Lapeyre G J, Lewenstein M and Acín A 2010 *Physical Review A* **81** 032327
- [43] Khanna S, Halder S and Sen U 2024 *Physical Review A* **109** 012419
- [44] Oh S M, Shin H, Marano S, Conti A and Win M 2024 Entanglement Percolation in Noisy Quantum Networks 2024 International Conference on Quantum Communications, Networking, and Computing (QCNC) pp 143–149
- [45] Vidal G 1999 *Physical Review Letters* **83** 1046–1049
- [46] Zangi S M, Shukla C, ur Rahman A and Zheng B 2023 *Entropy* **25** 1099–4300
- [47] Kesten H 1980 *Communications in Mathematical Physics* **74** 41–59
- [48] Latora V, Nicosia V and Russo G 2017 *Complex Networks: Principles, Methods and Applications* (Cambridge University Press)
- [49] Cuquet M and Calsamiglia J 2011 *Physical Review A* **83** 032319
- [50] Sykes M F and Essam J W 1964 *Journal of Mathematical Physics* **5** 1117–1127
- [51] Diaconis P 2005 *Notices of the American Mathematical Society* **52** 1348–1349 URL <https://math.stanford.edu/~cgates/PERSI/papers/what-is.pdf>
- [52] Życzkowski K, Penson K A, Nechita I and Collins B 2011 *Journal of Mathematical Physics* **52** 062201
- [53] Lloyd S and Pagels H 1988 *Annals of Physics* **188** 186–213
- [54] Hall M J 1998 *Physics Letters A* **242** 123–129
- [55] Li M, Liu R, Lü L, Hu M, Xu S and Zhang Y 2021 *Physics Reports* **907** 1–68
- [56] Leadbetter M R, Lindgren G and Rootzén H 1983 *Extremes and Related Properties of Random Sequences and Processes* (Springer)
- [57] Bianconi G and Dorogovtsev S N 2023 *arXiv* (arXiv:2305.12297)
- [58] Meng X, Gao J and Havlin S 2021 *Physical Review Letters* **126** 170501
- [59] Malik O, Meng X, Havlin S, Korniss G, Szymanski B K and Gao J 2022 *Communications Physics* **5** 193 ISSN 2399-3650
- [60] Meng X, Cui Y, Gao J, Havlin S and Ruckenstein A E 2023 *Physical Review Research* **5** 013225 ISSN 2643-1564 (arXiv:2110.04981)
- [61] Nath D and Roy S 2025 *arXiv* 2501.11004 (arXiv:2501.11004)

- [62] Albert R and Barabási A L 2002 *Reviews of Modern Physics* **74** 47–97
- [63] Boccaletti S, Latora V, Moreno Y, Chavez M and Hwang D U 2006 *Physics Reports* **424** 175–308
- [64] d Mata A S 2020 *Brazilian Journal of Physics* **50** 658–672
- [65] Duminil-Copin H 2017 *arXiv* (arXiv:1712.04651)
- [66] Grimmett G 1999 *Percolation (2nd edition)* (Springer)
- [67] Stauffer D and Aharony A 1992 *Introduction To Percolation Theory (2nd edition)* (Taylor & Francis)
- [68] Chitambar E, Leung D, Mančinska L, Ozols M and Winter A 2014 *Physical Review Letters* **328** 303–326
- [69] Nielsen M A and Chuang I L 2010 *Quantum Computation and Quantum Information (10th Anniversary Edition)* (Cambridge University Press)
- [70] Chitambar E and Gour G 2019 *Reviews of Modern Physics* **91** 025001
- [71] Nielsen M A 1999 *Physical Review Letters* **83** 436–439
- [72] Bhatia R 1997 *Matrix Analysis* (Springer)
- [73] Marshall A W, Olkin I and Arnold B C 2011 *Inequalities: Theory of Majorization and Its Applications (2nd Edition)* (Springer)
- [74] Nielsen M A and Vidal G 2001 *Quantum Information and Computation* **1** 76–93
- [75] Lewenstein M, Bruß D, Cirac J I, Kraus B, Kuś M, Samsonowicz J, Sanpera A and Tarrach R 2000 *Journal of Modern Optics* **47** 2481–2499
- [76] Lo H K and Popescu S 1999 *arXiv* (arXiv:quant-ph/9707038)

A. Basic Concepts of Networks and Percolation

Network theory provides a single theoretical and mathematical framework to describe a broad set of complex systems, ranging from biological networks of neurons in our brain to the network of social interaction or infrastructure networks like the power grid or the internet [62–64].

A network is described by a graph $G = (V, E)$, a mathematical structure consisting of two sets: V , the set of vertices in the graph, called “nodes”, and E , the set of “edges” connecting pair of nodes [38, 48].

The transport properties within a network or a lattice can be characterized using the mathematical framework of percolation theory [55]. In “edge percolation”, a coin is tossed for each of the edges of a network and with probability p the edge is kept, while with probability $1 - p$ the edge is removed. For small p , the majority of edges are eliminated, whereas for p close to 1, most edges are left intact. The system is said to “percolate” if a path of edges connecting opposite sides of the network exists [66].

A critical probability, known as the percolation threshold (p_c), defines a second order phase transition. For $p > p_c$, the system always percolates, meaning that a connecting path always exists, whereas for $p < p_c$ the system does not percolate. This transition is sharp for infinite networks (such as infinite lattices) while for finite systems you can study finite size effects at the transition point [67].

Defining percolation as connecting opposite sides of a network may be suitable for lattices, but it is non-trivial for more complex networks where it is not obvious what is a “side”. Because of that, one can use different order parameters. For instance, in this article, we have utilized the percolation strength P_∞ , which is defined as the probability

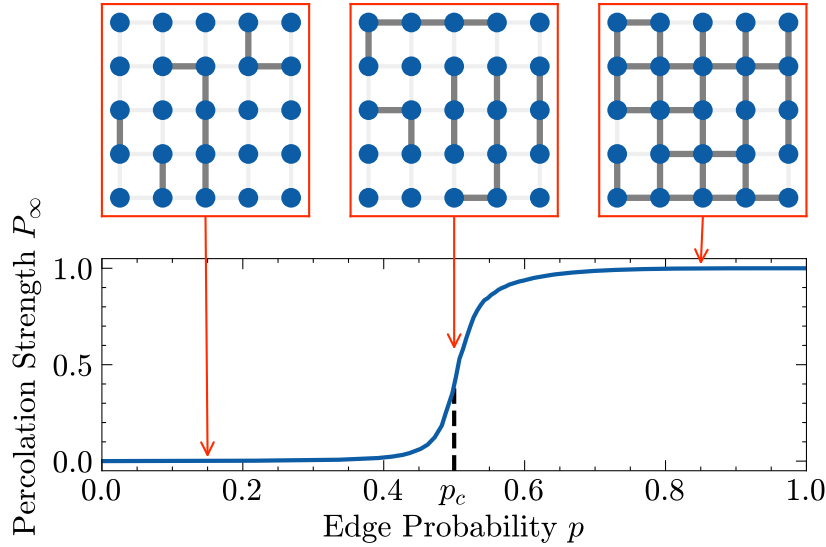


Figure A1: The plot shows an edge percolation simulation performed on a 100×100 square lattice. Three snapshot of an example of a simulation on a smaller lattice are shown for probabilities 0.15, 0.5, 0.85. The percolation transition is highlighted with $p_c^{\text{square}} = 1/2$ [47, 65].

that a node belongs to the largest connected component, that is, the cluster containing the largest amount of nodes in the network.

As shown in Figure A1, for low probabilities (below the transition) the network consists of small clusters, so $P_\infty(p < p_c) = 0$. But, above the percolation transition, the network will be completely connected and all the nodes will belong to the largest cluster, called the giant component, so $P_\infty(p > p_c) = 1$.

B. Entanglement Manipulation

Consider two distant laboratories A (Alice) and B (Bob). Both are allowed to perform local quantum operations in their respective systems, and can also send information to the other via classical manner (like, the telephone). Everything that can be decomposed only with these two actions falls under the umbrella of Local Operations and Classical Communication (LOCC) [68]. LOCC's are the free operation that uses entanglement as a resource, they cannot increase entanglement but they can transform it in various ways [69, 70].

In 1999 Nielsen [71] demonstrated a necessary and sufficient condition to convert deterministically a bipartite entangled state $|\psi\rangle$ into a bipartite entangled state $|\phi\rangle$ under LOCC.

The theorem states the following [71]: given a state with Schmidt decomposition $|\psi\rangle = \sum_{i=1}^d \sqrt{\lambda_i^\psi} |i\rangle_A \otimes |i\rangle_B$ where the Schmidt coefficients are put in decrescent order, i.e. $\lambda_1^\psi \geq \dots \geq \lambda_d^\psi$. It is possible to transform $|\psi\rangle$ into another bipartite state $|\phi\rangle$ using

LOCC iff $\lambda^\psi = (\lambda_1^\psi, \dots, \lambda_d^\psi)$ is “majorized” by λ^ϕ , i.e. $\lambda^\psi \prec \lambda^\phi$, where [72–74]:

$$\lambda^\psi \prec \lambda^\phi \quad \equiv \quad \sum_{i=1}^k \lambda_i^\psi \leq \sum_{i=1}^k \lambda_i^\phi \quad \text{for each } k = 1, \dots, d \quad (\text{B.1})$$

Nielsen theorem tells us that entanglement transformation is possible in a deterministic way using LOCC, but also that entanglement cannot be increased in this way.

For example, an operation that is allowed is entanglement distillation [75], which starts with N partially entangled states $|\psi\rangle^{\otimes N}$. These are distilled into a single, but more entangled state $|\phi\rangle$ § using LOCC as long as $\lambda^{\psi^{\otimes N}} \prec \lambda^\phi$.

Now, let’s say we want to convert a single bipartite state $|\psi\rangle$ to a more entangled state $|\phi\rangle$, in this case $\lambda^\psi \not\prec \lambda^\phi$ and we cannot achieve this deterministically using LOCC [68].

However, this can be achieved probabilistically using Stochastic LOCC (SLOCC) (also called “gambling with the entanglement”). In 1999 Vidal [45] generalized Nielsen theorem deriving the maximum probability to convert $|\psi\rangle \rightarrow |\phi\rangle$ with the optimal SLOCC protocol:

$$p(\psi \rightarrow \phi) = \min_{k=1, \dots, d} \frac{\sum_{i=k}^d \lambda_i^\psi}{\sum_{i=k}^d \lambda_i^\phi} \quad (\text{B.2})$$

When $|\phi\rangle = |\psi^-\rangle$ is a maximally entangled state of two qubits [76], the Schmidt coefficients are $\lambda_1^{\psi^-} = \lambda_2^{\psi^-} = 1/2$ and the Singlet Conversion Probability (SCP), that is, the probability to convert a generic 2-qubit state $|\psi\rangle \rightarrow |\psi^-\rangle$:

$$p(\psi \rightarrow \psi^-) = \min \left\{ \frac{\lambda_1^\psi + \lambda_2^\psi}{\frac{1}{2} + \frac{1}{2}}, \frac{\lambda_2^\psi}{\frac{1}{2}} \right\} = \min \left\{ 1, 2\lambda_2^\psi \right\} \quad (\text{B.3})$$

This conversion $|\psi\rangle \rightarrow |\psi^-\rangle$ can be implemented using the so-called “Procrustean method” [23]. Starting with the state $|\psi\rangle = \sqrt{\lambda_1}|00\rangle + \sqrt{\lambda_2}|11\rangle$ the method can be implemented with the following generalized measurement [34]:

$$M_1 = \begin{pmatrix} \sqrt{\frac{\lambda_2}{\lambda_1}} & 0 \\ 0 & 1 \end{pmatrix} \quad M_2 = \begin{pmatrix} \sqrt{1 - \frac{\lambda_2}{\lambda_1}} & 0 \\ 0 & 0 \end{pmatrix} \quad (\text{B.4})$$

For which, $M_1^\dagger M_1 + M_2^\dagger M_2 = \mathbb{1}$. The POVM outcomes are:

$$\begin{aligned} |\psi_1\rangle &= \frac{(M_1 \otimes \mathbb{1}) |\psi\rangle}{\sqrt{\langle \psi | (M_1^\dagger \otimes \mathbb{1})(M_1 \otimes \mathbb{1}) |\psi \rangle}} = |\psi^-\rangle \\ |\psi_2\rangle &= \frac{(M_2 \otimes \mathbb{1}) |\psi\rangle}{\sqrt{\langle \psi | (M_2^\dagger \otimes \mathbb{1})(M_2 \otimes \mathbb{1}) |\psi \rangle}} = |00\rangle \end{aligned} \quad (\text{B.5})$$

§ to be precise they are distilled into $|\phi\rangle \otimes_{i=1}^{N-1} |\eta_i\rangle$ where $|\eta_i\rangle$ are product states we can ignore

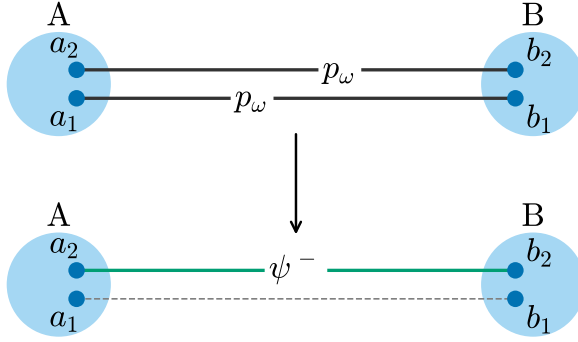


Figure C1: An example of a successful SLOCC protocol for a multiedge. Here, two identical states $|\omega\rangle$ are converted into a single maximally entangled state, the remaining state is just a product state.

With the following probabilities:

$$\begin{aligned} p(|\psi^-\rangle) &= 2\lambda_2 \\ p(|00\rangle) &= 1 - 2\lambda_2 \end{aligned} \tag{B.6}$$

The SCP p_ψ is defined as $p(|\psi^-\rangle)$, the probability of projecting $|\psi\rangle$ into $|\psi^-\rangle$. With probability $p(|00\rangle) = 1 - p_\psi$ we are left with no entanglement at all.

This SCP can also be understood as an entanglement measure: maximally entangled states have an SCP of 1 while separable states have an SCP of 0.

C. Multigraph quantum networks

The initial setup to implement the q -swap operation described in Section 2.2 is a network sharing multiple bipartite entangled states between users, i.e. a ‘‘Multigraph quantum network’’ [38].

Starting with two identical state $|\omega\rangle$ one can apply the SLOCC purification method like in Figure C1 in multiple ways:

- One can convert the two initial states separately and asks what is the probability that at least one is successful. Then we will have that $p_{\text{sep}} = 1 - (1 - p_\omega)^2 = 2p_\omega - p_\omega^2$ [31].
- We can implement the optimal SCP from Equation (B.2), with probability:

$$p(\omega \otimes \omega \rightarrow \psi^-) = 2(1 - (\lambda_1^\omega)^2) = 2(1 - (1 - \lambda_2^\omega)^2) = 2p_\omega - \frac{p_\omega^2}{2} \tag{C.1}$$

We will call this 2-state distillation SCP $p_{\omega \otimes 2}$. This result is generalized to the case of N -state distillation as $p_{\omega \otimes N} = 2(1 - (\lambda_1^\omega)^N)$.

For example, if we want to calculate the CEP for a double-bond network then we will have that $p_{\omega \otimes 2} = p_c$. So, we get that the minimum amount of entanglement for each



Figure D1: Examples of a multiedge in a random state network. Here, two edges connects node A with node B . (a) For “equal multiedge” we will have that only one probability p_k is drawn from the distribution and assigned to all the edges inside a multiedge. (b) For “independent multiedge” we have that all the edges inside a multiedge are drawn from the distribution.

copy of the initial state is:

$$p_{2\text{-network}}^{\text{CEP}} = 2 - \sqrt{4 - 2p_c} \quad (\text{C.2})$$

Which, as we expect, is always lower than the CEP for a single network which is just $p_{1\text{-network}}^{\text{CEP}} = p_c$ (less initial entanglement per state is needed).

D. Multigraph random quantum networks

As in the case of entanglement percolation in standard networks, we are still allowed to have multiple states from one node to another as in Equation (C.1). We will now have a “Multigraph Random quantum network”. With this new model we have to distinguish two possible cases:

- **Equal multiedge:** all the (random) edges connecting the same two users are equal, as shown in Figure D1a. Here, the SLOCC purification probability will be:

$$p(\psi_k^{\otimes 2} \rightarrow \psi^-) = p_{k^{\otimes 2}} = \min \left\{ 1, 2 \left[1 - \left(\lambda_1^{\psi_k} \right)^2 \right] \right\} \quad (\text{D.1})$$

- **Independent multiedge:** all the edges are independently drawn from the distribution of the SCPs, as shown in Figure D1b. The SLOCC probability in this case is:

$$p(\psi_{k_1} \otimes \psi_{k_2} \rightarrow \psi^-) = p_{k_1 \otimes k_2} = \min \left\{ 1, 2 \left(1 - \lambda_1^{\psi_{k_1}} \lambda_1^{\psi_{k_2}} \right) \right\} \quad (\text{D.2})$$

We can write both these equation as a function of the SCP $p_k = 2\lambda_2^{\psi_k}$ in the following way:

$$\begin{aligned} p_{k^{\otimes 2}} &= 2p_k - \frac{p_k^2}{2} \\ p_{k_1 \otimes k_2} &= p_{k_1} + p_{k_2} - \frac{p_{k_1}p_{k_2}}{2} \end{aligned} \quad (\text{D.3})$$

We can then average these results out to obtain:

$$\begin{aligned} \langle p_{k^{\otimes 2}} \rangle &= 2\langle p \rangle - \frac{\langle p^2 \rangle}{2} \\ \langle p_{k_1 \otimes k_2} \rangle &= 2\langle p \rangle - \frac{\langle p \rangle^2}{2} \end{aligned} \quad (\text{D.4})$$

We will always have $\langle p^2 \rangle \geq \langle p \rangle^2$ so at the end we conclude that:

$$\langle p_{k_1 \otimes k_2} \rangle \geq \langle p_{k \otimes 2} \rangle \quad (\text{D.5})$$

The average SLOCC probability of having the multiple states all randomly distributed is always higher than the case of repeated multiedges. Therefore, we conclude that the random multiedge is always better than the repeated multiedge.